ISSN: 2096-3246
Volume 57, Issue 02, August, 2025

DESIGN AND ANALYSIS OF A DOUBLE-SIDED LIM

Praful Nandankar[1], Jyoti Prashant Rothe[2], Archana Girish Shirbhate[3], Snehal Pravin Pachpor[4], Rashmi A. Keswani[5]

[1] Assistant Professor, Department of Electrical Engineering, Government College of Engineering, Nagpur, India – pppful@gmail.com

[2] Professor, Department of Electrical Engineering, St. Vincent Pallotti College of Engineering & Technology, Nagpur, India – jrothe@stvincentngp.edu.in

[3] Associate Professor, Department of Electrical Engineering, Anjuman College of Engineering & Technology, Nagpur-ashirbhate@anjumanengg.edu.in

[4] Associate Professor, Department of Electrical Engineering, Bajaj Institute of Technology, Wardha- snehal.pachpor@bitwardha.ac.in

[5]Associate Professor, Department of Electrical Engineering, Priyadarshini College of Engineering, Nagpur- rashmi.keswani@pcenagpur.edu.in

Abstract –A double-sided linear induction motor (DSLIM) optimised for high-thrust and high-efficiency applications in automation and transportation is designed, analysed, and simulated in this work. With its symmetrical double-sided design, the DSLIM offers balanced magnetic flux and increased thrust density, which makes it appropriate for automated material handling and high-speed urban transit systems like Maglev trains. Finite Element Analysis (FEA) is used to analyse performance and calculate important parameters such as thrust force, synchronous speed, and slip. According to simulation results, the DSLIM design is effective. It produces a lot of thrust, is around 70% efficient at the ideal slip levels, and significantly reduces end effects, which are major problems in LIM applications. The design's precision and dependability are confirmed by the high degree of agreement between theoretical calculations and simulation results.

Keywords- Double-Sided LIM (DSLIM), Finite Element Analysis (FEA), Thrust Force, End Effects, Magnetic Flux Distribution, Urban Transit Systems

1. Introduction

Linear Induction Motors (LIM) is a specific type within the induction motor family, where movement is produced lacks a rotary component (linear), providing benefits for applications requiring linear force as opposed to rotary motion. LIMs, which function based on the principles of electromagnetic induction, produce a moving magnetic field within the primary winding that induces currents into the secondary unit. The action creates linear propulsion while the interaction is one-dimensional, which makes LIMs ideal in applications associated with high-speed transport, automated material handling and industrial processes.

LIMs require no rotating parts, they have no rotary motors and, therefore, a more straightforward design offering fewer maintenance needs while enabling high-precision motion control not possible with traditional rotary motors. Its motor structure can be single-sided or double-sided. The latter also delivers more linear thrust and greater force density suited for applications such as Maglev trains and urban transit systems. Abdollahi et al. introduced a double-sided LIM design that exhibited excellent potential performance, especially for transportation applications where high efficiency and

effectiveness in load and speed variations are required [1], [2].

In this paper, a flat double-sided LIM that aims to optimise performance traits for transportation applications is designed and analysed. The study uses simulations to assess magnetic flux distribution, thrust force, and efficiency for operating conditions to conceptualise existing challenges as well as the potential of LIM for future high-speed transit and industrial automation issues

2. Literature Review

The advancement of research on Linear Induction Motors (LIM) has come up to a new level, especially for high-speed transportation and automation applications. Initial research interest in LIMs was based on their relatively simple design and the potential to generate linear motion without intermediate mechanical components. Significant improvements in LIM design, analysis and application over the past few years have tackled the important issues of efficiency, thrust force and exit effects.

Rajan et al. examined the mathematical modelling of LIMs, with an emphasis on high-acceleration applications such as spacecraft propulsion and urban rail systems. The primary use of LIMs demonstrated by the study is high velocity, which is made feasible by the simple stator construction of LIMs and the possibility of producing a large linear force. First of all, the performance curves presented enable one to understand how the LIMs operate in general terms and are necessary for additional design improvements [3], [4].

Due to their high force density and simple track structure, Double-sided Linear Induction Motors (DSLIMs) are suitable replacements for urban transportation systems. Abdollahi et al., using an analytical model validated at high speeds (2015) showed that a DSLIM design for an air-bus system was effective in suppressing longitudinal and transverse edge effects. In another work, Lee and Chin (1979) proposed a quasi-three-dimensional model to limit end effects by staggering the excitatory windings of the LIM and calculating the equivalent secondary resistance more acutely to improve LIM performance. The optimisation lines of research on LIMs have primarily investigated efficiency and adaptability for industrial and transportation applications. Solomin et al. (2019) modelled secondary currents for magnetic levitation systems. Hasan et al. (2015) focused on torque maximisation and energy loss reduction for industrial applications. LIMs have also been successfully used in Maglev and high-speed transport systems, as reported by Laithwaite (1969) and Lu et al. (2013), further enforcing their role in sustainable and efficient urban transport. In particular, these studies highlight the optimisation of performance capabilities in transportation and industrial-relevant domains such as end effects handling, efficiency improvement potential, and thrust performance [5].

3. Principle of Operation

Fig. 3.1 shows the main component (which is also known as the stator) is a stationary part which has a sequence of windings along a linear structure. These windings are driven by a three-phase AC power supply, which creates a travelling magnetic field running the length of the primary. This secondary (a bit like the rotor in rotary motors) is a metal or copper conductor plate disposed opposite to the primary. - Double-sided LIM (DSLIM): There are two primary windings on either side of the secondary to increase the force density and performance in applications such as high-speed rail and urban transit. A travelling magnetic field is created when a three-phase AC passes through the stator's

primary windings and travels the entire length. Eddy currents are created in the conductive secondary element by this moving field.

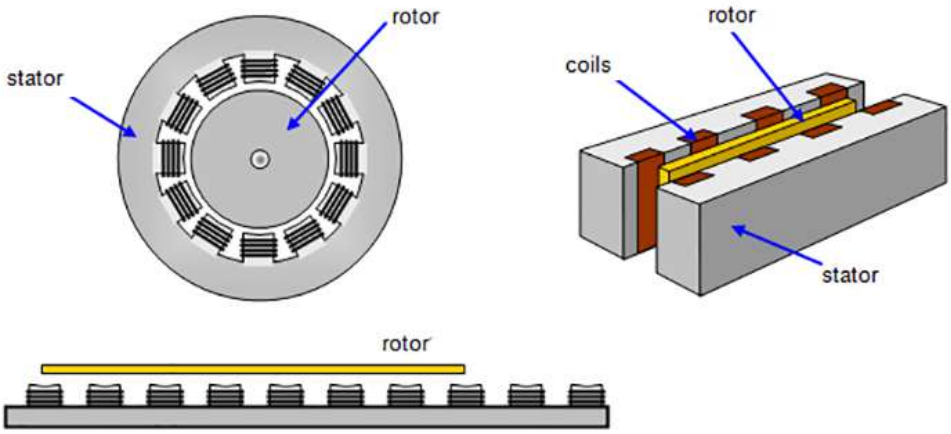

Fig. 3.1 Stator, Rotor and Coil designs of conventional linear Induction motors

The induced currents in Fig. 3.2 produce their magnetic field, which interacts with the moving field to produce a linear thrust force along the magnetic field's direction, per Lenz's Law. The current in the primary windings, the slip (difference between the magnetic field's primary and secondary speeds), and the pole pitch are some of the variables that affect how much force is there. Similar to traditional induction motors, LIM efficiency is influenced by the slip value; optimal performance is achieved at particular slip ranges that differ depending on the application [7], [8].

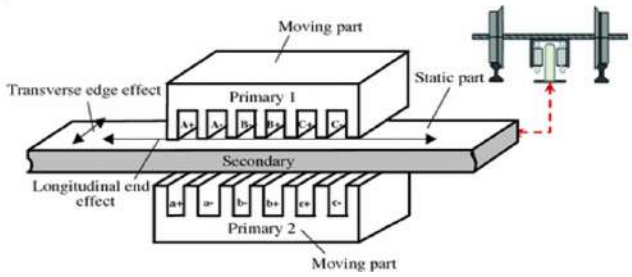

Fig. 3.2 LIM while driving an application

The finite length of the primary windings causes end effects, which are unique to LIMs and result in an uneven distribution of the magnetic field. At high speeds, these effects become more noticeable and can result in energy losses by decreasing the effective thrust. These problems were addressed by Abdollahi et al. in their design of a double-sided LIM, suggesting that considering longitudinal and transverse edge effects might greatly enhance LIM performance in high-speed applications. Due to their direct linear thrust and lack of rotating parts, LIMs are ideal for high-speed and precise applications because they decrease mechanical wear and require less maintenance. These qualities allow LIMs to perform very well in a variety of applications where dependability, speed, and seamless operation are critical, including automated material handling systems, airport shuttles, and Maglev trains

4. Design Calculations

One of the most important parameters in a LIM is the synchronous speed (Vs) of the travelling magnetic field, which is affected by the supply frequency (f) and pole pitch (τ). The following formula can be used to compute it:

$$V_S = 2\pi f \quad (1)$$

where f is the supply frequency in Hertz (Hz) and τ is the pole pitch in meters.

In relation to the synchronous speed, the slip s is the difference between the synchronous speed and the secondary's actual speed V. The slip is computed as follows:

$$s = \frac{Vs - V}{Vs} \quad (2)$$

where V is the secondary's speed.

High thrust production and effective energy transfer can be attained by maximizing the slip value. To maintain an ideal slip range, which directly affects the thrust and efficiency performance of the LIM, modifications were made to the pole pitch and supply frequency in this design.

The LIM's thrust force (F) is determined by the motor's power supply (P), synchronous speed (Vs), and slip (s). This gives the push force:

$$F = \frac{P}{V_S} * (1 - s) \quad (3)$$

where Vs is the synchronous speed (m/s), s is the slip, and P is the power provided to the LIM in watts (W).

The force calculation additionally takes into account the dual primary structure's increased surface area and effective magnetic field for the double-sided LIM design, which increases thrust density. According to the study of Abdollahi et al., this arrangement permits higher force production, which is particularly advantageous in high-speed applications.

The following is an expression for the LIM's efficiency η:

$$\eta = \frac{P_m}{P} = 1 - s \quad (4)$$

In this case, Pm represents the LIM's torque output. Reduced slip results in less energy being lost through resistive losses, which boosts efficiency. Nevertheless, the thrust diminishes at very low slips, resulting in a compromise between force production and efficiency.

The LIM's inductive and resistive components have an impact on the power factor cos ϕ, another crucial metric. Through modelling, power factor and efficiency were adjusted to reach values that support high-performance operations with low losses.

5. Limitations and Future Research Directions

The Linear Induction Motor (LIM) was designed and simulated to maximize important performance attributes like thrust, efficiency, and end-effect handling. Because of its symmetrical form and increased force density, a double-sided LIM (DSLIM) was selected for this investigation. These features are advantageous for applications involving industrial automation and high-speed transportation. Establishing the primary and secondary configurations of the motor, choosing appropriate materials, and figuring out its electrical and magnetic characteristics were all part of the design phase. The operational behaviour of the motor was then examined and these parameters were validated through simulation using Finite Element Analysis (FEA).

5.1 Double-Sided LIM Design: Design parameters, including supply frequency, air gap, and pole pitch, were computed to get the required synchronous speed and slip in order to maximize performance. Achieving the required thrust for high-speed operation and preserving effective energy transfer depends on this. Furthermore, the motor's air gap was reduced to improve magnetic coupling,

and the pole pitch was modified to meet the slip requirements for different operating loads.

5.2 Simulation Setup: The electromagnetic behaviour of the LIM was simulated using Finite Element Analysis (FEA), with an emphasis on important metrics such as thrust, power factor, and magnetic flux distribution. The FEA configuration comprised:

Magnetic Field Distribution: To replicate the magnetic flux distribution of the LIM and demonstrate the interaction between the moving magnetic field and the secondary, a two-dimensional model was developed. Areas of high force generation were highlighted by the simulation's visual depiction of flux density across the motor.

Evaluation of Thrust Force: By calculating thrust force at various slip values and current inputs, the simulation made it possible to evaluate how well the LIM performed in various scenarios. The motor's usefulness for applications needing a high force density was supported by the dual-sided configuration's increased thrust outputs and uniform force distribution over the secondary.

Analysis of End Effects: By looking at the flux distribution at the ends of the major windings, end effects—a frequent problem in LIMs, especially at high speeds—were examined. By distributing the magnetic field evenly on both sides of the secondary, the DSLIM's design lessened end effects, producing a steadier thrust production and fewer losses at the margins.

The performance of the LIM was thoroughly examined by the FEA simulation, which nearly matched theoretical computations. Peak flux densities matched areas of highest force generation, indicating a consistent magnetic flux distribution throughout the DSLIM, according to the simulation.

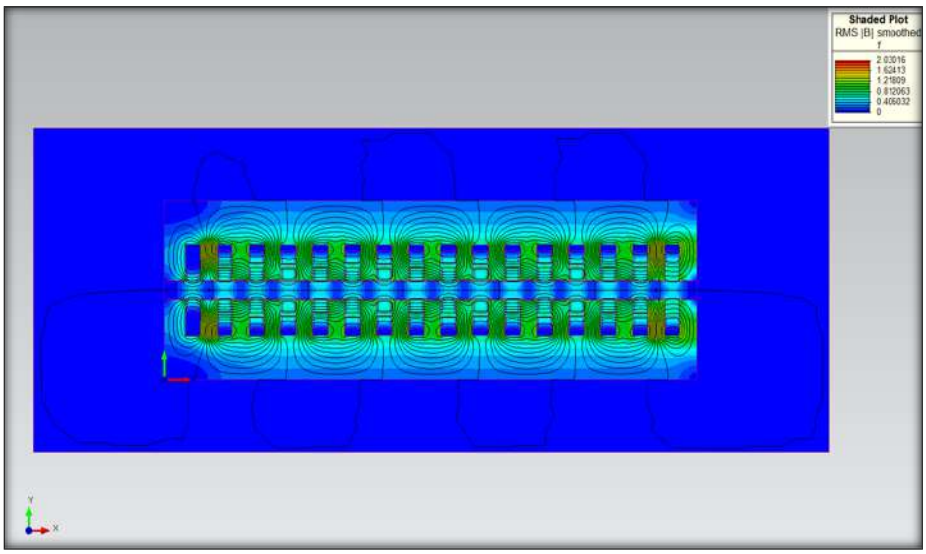

Fig. 5.1 Magnetic field density representation over the entire body

As the theoretical model predicted, a larger effective thrust was made possible by the double-sided structure, which also decreased flux leakage. At modest slip levels, the thrust force reached its ideal values as it rose proportionately with the current. These slip values were also found to be where efficiency peaked, confirming the slip and synchronous speed calculations. Under optimal circumstances, the double-sided LIM's efficiency reached about 70%, and its power factor was above 0.8.

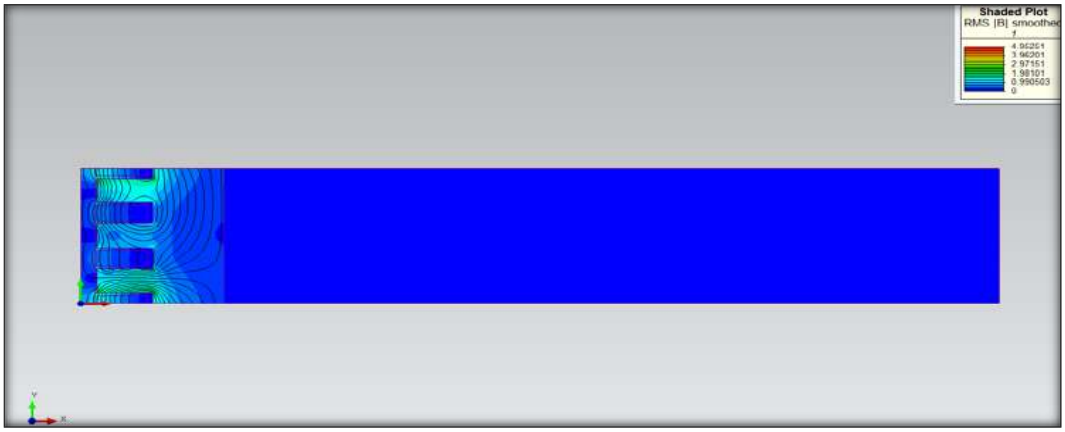

Fig. 5.2 Magnetic field density view of ¼ proposed simulation model

To eliminate the end effects that usually lower thrust in LIMs, the DSLIM balanced the magnetic field on both sides of the secondary. The FEA simulation confirmed that the double-sided design successfully reduces end effects, even at high speeds, by displaying a uniform flux distribution close to the primary's edges as shown in Fig. 5.1 and Fig. 5.2.

In comparison to single-sided LIM setups, the results show that the DSLIM design offers improved thrust, efficiency, and fewer end effects. According to these results, the DSLIM configuration may successfully satisfy the requirements of high-speed and high-force applications, including automated material handling systems, Magnetic Levitation (Maglev) trains, and urban transportation options.

6. Simulation Results of H Adaptation Technique

The H adaption method, also known as h-refinement, is a technique used to increase the accuracy of numerical solutions such as the Finite Element Method (FEM) and the Boundary Element Method (BEM). The goal of h-adaptation is to reduce discretization error in areas of the computational domain where it is expected to be significant. This mechanism is accomplished by lowering the size (h) of the mesh components in specified error-prone locations. Instead of utilising a uniform mesh with same same-sized elements everywhere, h-adaptation generates a mesh with smaller elements as needed. The benefits of H Adaptation are improved accuracy, computational efficiency and improved resolution of local features.

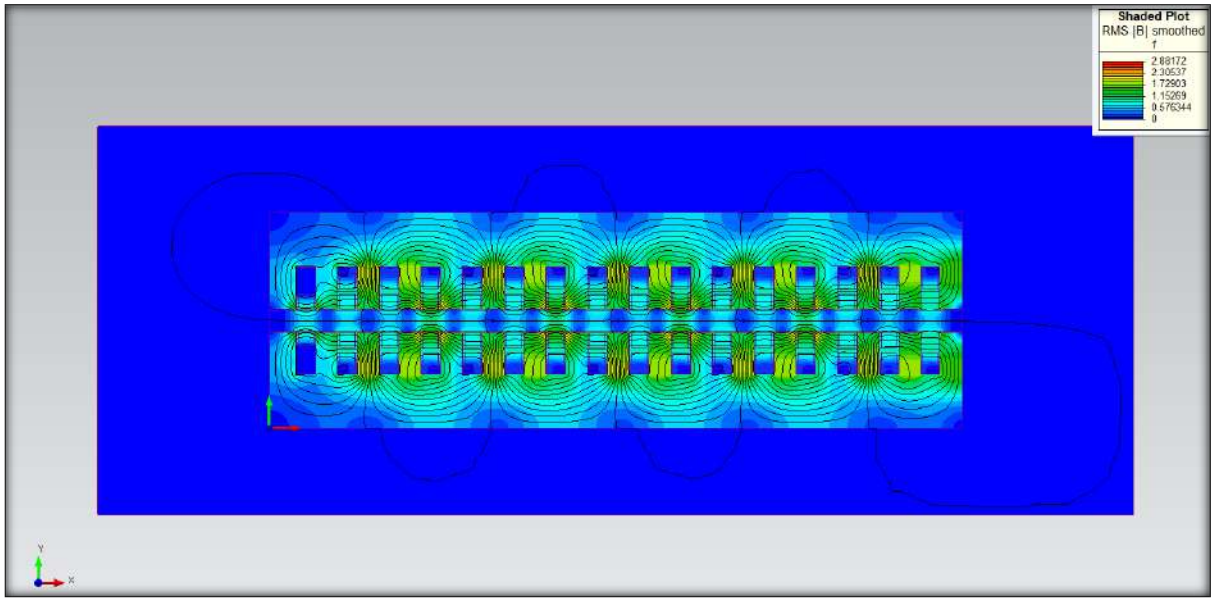

Fig. 6.1 Simulation results of Double-sided LIM with H-Adaptation

Body	**Force**				**Torque**			
ID Components	**X**	**Y**	**Z**	**Magnitude**	**X**	**Y**	**Z**	**Magnitude**
Stator 1	-1.04	-60.3	0	60.3	0	0	-12.1	12.1
Stator 2	-1.04	60.3	0	60.3	0	0	12.2	12.2
Rod	2.19	1.56E-05	0	2.19	0	0	-0.137	0.137

Fig. 6.1 illustrates the outcome of applying the H adaptation method to a Double-Sided Linear Induction Motor (DSLIM). This technique enhances simulation precision by refining the mesh in regions where the magnetic field is stronger. In the image, a colour plot visualises magnetic flux density (|B|), with various colours representing different intensity levels. The magnetic field is most concentrated around the stator teeth, indicating effective interaction between the stator and the rod. According to the force data presented in the table, Stator 1 and Stator 2 experience equal and opposite forces along the Y-axis. Stator 1 has a force of -60.3 N, while Stator 2 has +60.3 N, suggesting that both are exerting force in opposite directions with the same magnitude. This symmetrical force distribution is crucial for stable operation and ensures that the rod receives a consistent push in the desired direction. The rod itself experiences a force of approximately 2.19 N in the X-direction, which corresponds to the intended linear movement. Regarding torque, both stators again display nearly equal but opposite torque values in the Z-direction—12.1 Nm for Stator 1 and 12.2 Nm for Stator 2. This balance indicates there is no unwanted rotational motion, showing that the system remains well-stabilised. The rod experiences only a minimal torque of about 0.137 Nm, demonstrating that most of the energy is being directed towards linear movement, which aligns with the purpose of this motor design. These results confirm that the H adaptation method significantly enhances the accuracy of magnetic field computations and demonstrates that the DSLIM functions

in a balanced and efficient way.

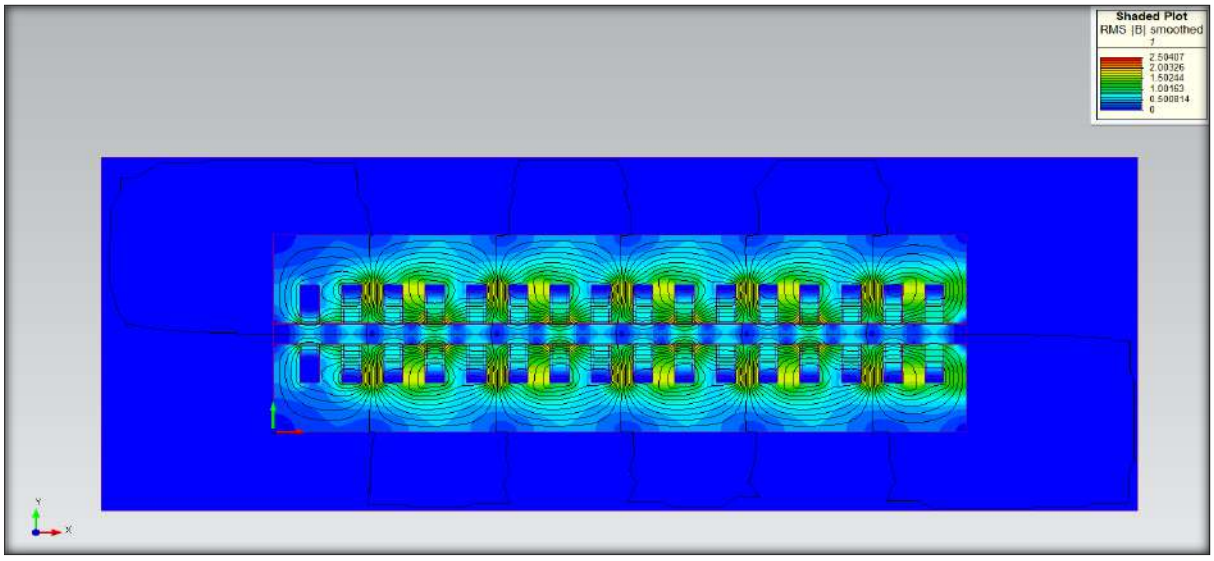

Fig. 6.2 Simulation results of Double-sided LIM without H-Adaptation

Body	**Force**				**Torque**			
ID Components	**X**	**Y**	**Z**	**Magnitude**	**X**	**Y**	**Z**	**Magnitude**
Stator 1	-0.997	-60.7	0	60.7	0	0	-12.2	12.2
Stator 2	-1.07	60.7	0	60.7	0	0	12.3	12.3
Rod	2.19	-0.000909	0	2.19	0	0	-0.137	0.137

The simulation results for the Double-Sided Linear Induction Motor (DSLIM) without using the H adaptation technique are shown above in Fig. 6.2. In this scenario, the computational mesh hasn't been refined based on magnetic field intensity, which could impact the accuracy of the magnetic field calculations. The shaded plot still illustrates magnetic flux density (|B|), with the highest intensity observed near the stator teeth. However, the magnetic field lines appear less smooth than in the H-adapted model, potentially affecting the precision of force and torque computations. Reviewing the data table, Stator 1 and Stator 2 again produce almost equal and opposite forces along the Y-axis (−60.7 N and +60.7 N), confirming that the motor is operating in a balanced state. The rod experiences a net force of approximately 2.19 N in the X-direction, indicating it continues to move as intended, similar to the case with H adaptation. When it comes to torque, both stators generate nearly opposite torques in the Z-direction (−12.2 Nm and +12.3 Nm), suggesting well-balanced electromagnetic behaviour. The rod itself experiences only a small torque of 0.137 Nm, which is comparable to the H-adapted scenario, showing that most of the energy is effectively used for linear movement rather than rotation. In summary, even without H adaptation, the motor still performs effectively, though with potentially reduced accuracy due to the unrefined mesh. This can lead to slight variations in the measured forces and torques. Implementing H adaptation can enhance simulation precision by allocating computational effort to the regions that influence performance the most.

7. Dimensions of Double-Sided LIM

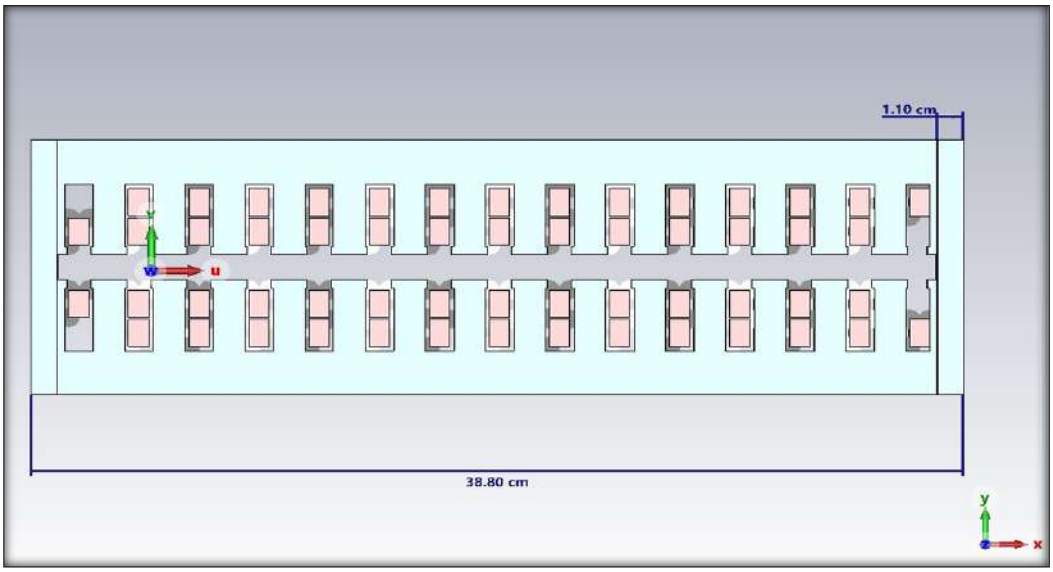

(a)

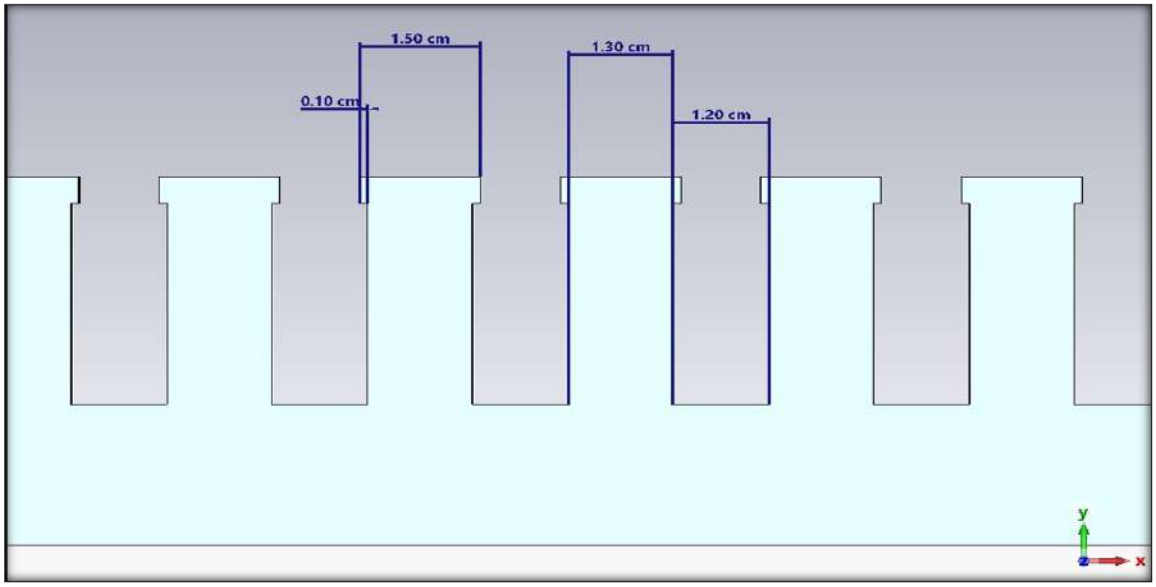

(b)

Fig.7.1 Front View

The front view of the double-sided LIM has been shown in Fig. 7.1. Fig. 7.1 (a) shows the dimensions of the motor, which includes the full length of the motor and Fig. 7.1 (b) shows the dimensions of the motor's teeth and the spacing between the teeth. The coils of the motors are also seen in the first image. The teeth are not perfectly made rectangles; rather, it's made with a little extension of 0.10 cm to keep the coils intact in their positions. The components used to keep the two sides of the

stator intact can be seen in Fig. 7.1(a), which has been marked with the dimension of 1.10 cm.

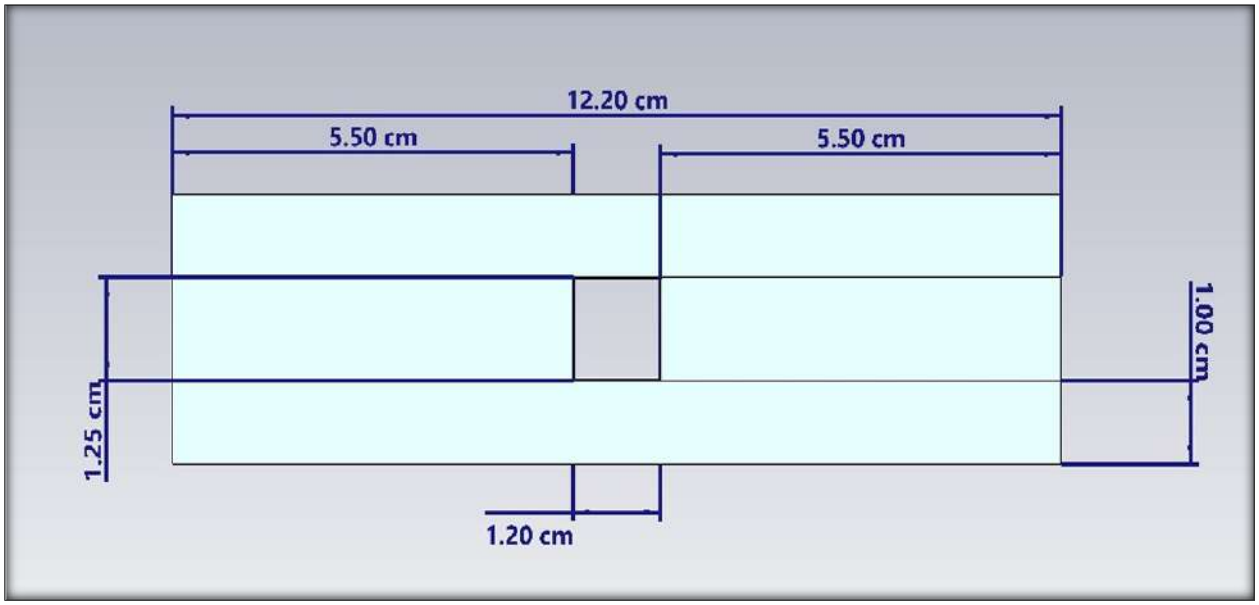

Fig. 7.2 Back view

In Fig. 7.2, the dimensions of the motor from the back view are shown. The square shape seen in the centre of the image is where the rod of the motor goes. The rod moves back and forth in this air gap only. The main motor is the centre one, which has a thickness of 1.25 cm, and the above and below components are the assembly components to keep the two sides of the stator intact.

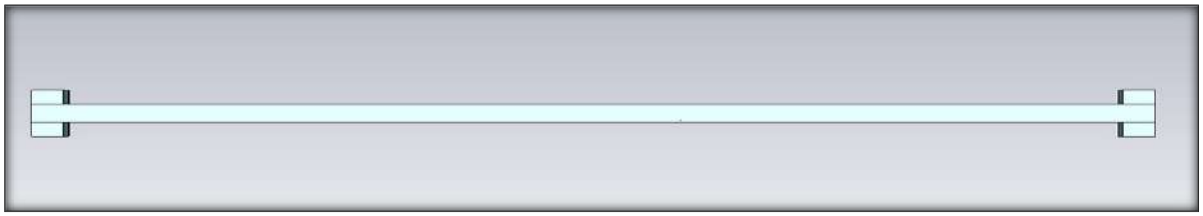

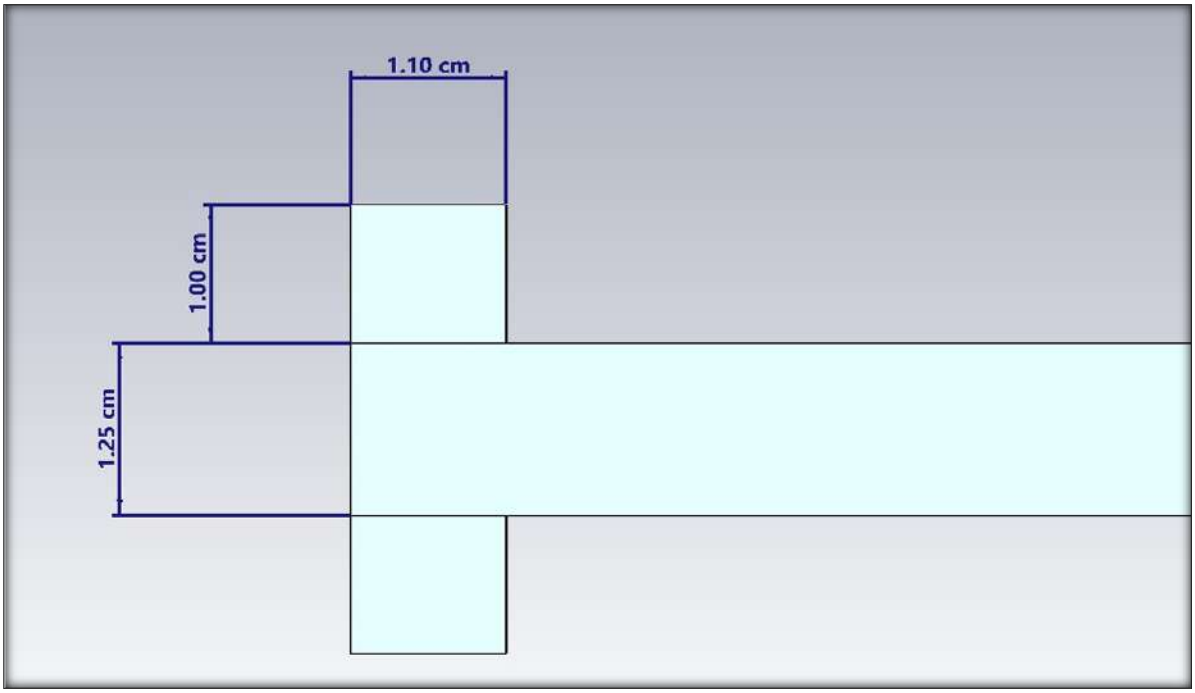

Fig. 7.3 Side View

This is the side view of the double-sided linear induction motor. It shows the dimensions that are required along the side of the motor. The main body of the motor has a thickness of 1.25 cm, and the shape, which has the dimensions of 1.10 x 1.00 cm, is nothing but an assembly to keep the two sides of the stator in a fixed position.

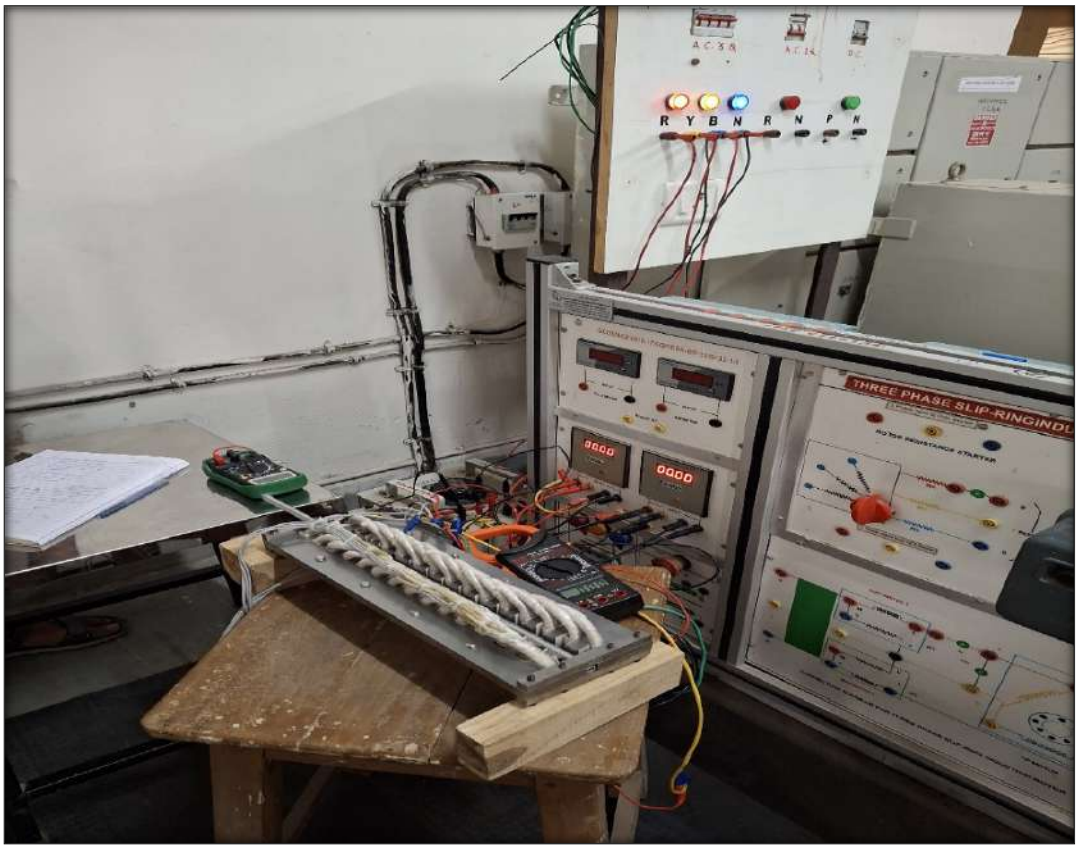

Fig. 7.4 Experimental prototype of the proposed Double-sided LIM

Fig. 7.4 shows an experimental prototype setup, likely developed to test and analyse the performance of a Double-Sided Linear Induction Motor (DSLIM). At the centre of the image, placed on a wooden stand, is the main testing component, which appears to be a metallic reaction rail (often aluminium) surrounded by coil windings. These coils are arranged to simulate the stator sections of the DSLIM, which work together to generate a linear electromagnetic force when energised. To the right, a well-equipped control and measurement panel can be seen. This panel includes digital voltmeters and ammeters that are used to monitor phase voltages and currents during the experiment. Above the panel, a phase indicator section displays the status of the three-phase supply, marked by red (R), yellow (Y), and blue (B) lights. These indicators help ensure the system is properly energised and balanced. Overall, this experimental arrangement allows for practical testing of electromagnetic thrust, torque, and current behavior under controlled conditions.

8. Conclusion

The Double-Sided Linear Induction Motor (DSLIM) designed and analyzed in this study demonstrated high-performance capabilities, especially in applications demanding significant thrust and efficiency. Through Finite Element Analysis (FEA), the DSLIM achieved a thrust force of approximately 2.19 N on the rod, while each stator generated equal and opposite forces of around ±60.3 N in the Y-direction, ensuring balanced and stable operation. The torque measurements revealed that both stators produced nearly equal and opposite torques of ±12.1 Nm, and the rod itself experienced a minimal torque of about 0.137 Nm, confirming the system's suitability for linear, rather than rotational, motion. These values remained consistent even when the H adaptation technique was applied, enhancing the simulation's precision by refining the mesh in regions of high magnetic intensity. Under optimal conditions, the motor exhibited an efficiency of approximately 70% and a power factor greater than 0.8, affirming the DSLIM's effectiveness in converting electrical energy into linear motion with minimal losses. The symmetrical design of the stators significantly reduced magnetic end effects and flux leakage, which are common challenges in conventional LIMs. The simulation results closely matched theoretical predictions, validating the design process and confirming the DSLIM's potential for high-speed transportation systems like Maglev trains and automated industrial applications. These findings suggest that with further optimization, such as material improvements and control strategies, the DSLIM can become a core component in next-generation linear drive systems.

References

[1] R. Thornton, M. T. Thompson, B. M. Perreault, and J. Fang, "Linear motor-powered transportation [Scanning the Issue]," Proceedings of the IEEE, vol. 97, pp. 1754-1757, 2009.

[2] W. Li, T.W. Ching and K. T. Chau, "A Hybrid-Excited Vernier Permanent-Magnet Machine Using Homopolar Topology, " IEEE Transactions on Magnetics, Vol. 53, No. 11, Article#: 8111507, 2017.

[3] G. Lv, T. Zhou, and D. Zeng, "Influence of the Ladder-Slit Secondary on Reducing the Edge Effect and Transverse Forces in the Linear Induction Motor," IEEE Transactions on Industrial Electronics, vol. 65, no. 9, pp. 7516–7525, 2018, doi: 10.1109/TIE.2018.2795525.

[4] W. Liu, Z. Cui, W. Hao, and L. Song, “Effect of static longitudinal end effect on performance of arc linear induction motor,” 2019, doi: 10.1109/ICEMS.2019.8922324.

[5] G. Wang, Y. Wang, J. Xu, N. Zhao, and D. Xu, “Weight-Transducerless Rollback Mitigation Adopting Enhanced MPC with Extended State Observer for Direct-Drive Elevators,” IEEE Transactions on Power Electronics, vol. 31, no. 6, pp. 4440–4451, 2016, doi: 10.1109/TPEL.2015.2475599.

[6] E.-J. Park, S.-Y. Jung, and Y.-J. Kim, "A Design of Optimal Interval between Armatures in Long Distance Transportation PMLSM for End Cogging Force Reduction," Journal of Electrical Engineering and Technology, vol. 11, pp. 361-366, 2016.

[7] F. Daldaban and N. Ustkoyuncu, "A novel linear switched reluctance motor for railway transportation systems," Energy Conversion and Management, vol. 51, pp. 465-469, 2010.

[8] Lv, G.; Zeng, D.; Zhou, T. An Advanced Equivalent Circuit Model for Linear Induction Motors. IEEE Trans. Ind. Electron. 2018, 65, 7495–7503.

[9] Kircher, R.; Klühspies, J.; Palka, R.; Fritz, E.; Eiler, K.; Witt, M. Electromagnetic Fields Related to High-Speed Transportation Systems. Transp. Syst. Technol. 2018, 4, 152–166.

[10] Sotelo, G.G.; Sass, F.; Carrera, M.; Lopez-Lopez, J.; Granados, X. Proposal of a Novel Design for Linear Superconducting Motor Using 2G Tape Stacks. IEEE Trans. Ind. Electron. 2018, 65, 7477–7484.

[11] Woronowicz, K.; Palka, R. Optimised Thrust Control of Linear Induction Motors by a Compensation Approach. Int. J. Appl. Electromagn. Mech. 2004, 19, 533–536.

[12] Woronowicz, K.; Palka, R. An advanced linear induction motor control approach using the compensation of its parameters. In Electromagnetic Fields in Electrical Engineering; IOS Press: Amsterdam, The Netherlands, 2002; pp. 335–338.

[13] D. Y. Kim, M. R. Park, J. H. Sim, and J. P. Hong, “Advanced Method of Selecting Number of Poles and Slots for Low-Frequency Vibration Reduction of Traction Motor for Elevator,” IEEE/ASME Transactions on Mechatronics, vol. 22, no. 4, pp. 1554–1562, 2017, doi: 10.1109/TMECH.2017.2695059.

[14] K. Al-Kodmany, “Tall buildings and elevators: A Review of Recent Technological Advances,” Buildings, vol. 5, no. 3, pp. 1070–1104, 2015, doi: 10.3390/buildings5031070.

[15] B. Knežević, B. Blanuša, and D. Marčetić, “Model of elevator drive with jerk control,” 2011, doi: 10.1109/ICAT.2011.6102118.

[16] S. Masoudi, H. Mehrjerdi, and A. Ghorbani, “New elevator system constructed by multi-translator linear switched reluctance motor with enhanced motion quality,” IET Electric Power Applications, vol. 14, no. 9, pp. 1692–1701, 2020, doi: 10.1049/iet-epa.2019.0996.

[17] S. Masoudi, M. R. Feyzi, and M. B. B. Sharifian, “Force ripple and jerk minimization in double-sided linear switched reluctance motor used in elevator application,” IET Electric Power Applications, vol. 10, no. 6, pp. 508–516, 2016, doi: 10.1049/iet-epa.2015.0555.

[18] D. Wang, C. Shao, and X. Wang, “Performance Analysis and Design Optimization of an Annular Winding Bilateral Linear Switch Reluctance Machine for Low-Cost Linear Applications,” IEEE Transactions on Applied Superconductivity, vol. 26, no. 7, 2016, doi: 10.1109/TASC.2016.2595584.

[19] T. Higuchi, Y. Yokoi, T. Abe, N. Yasumura, Y. Miyamoto, and S. Makino, “Design analysis of a segment type linear switched reluctance motor,” 2017, doi: 10.23919/LDIA.2017.8097226.

[20] N. A. M. Nasir, F. A. Shukor, N. M. Zuki, and R. N. F. K. R. Othman, “Design of the segmented-type switched reluctance linear synchronous motor (SSRLSM) for domestic lift application,” Progress In Electromagnetics Research C, vol. 108, pp. 13–22, 2021, doi: 10.2528/PIERC20110205.

[21] W. Zhao, M. Cheng, J. Ji, R. Cao, Y. Du, and F. Li, "Design and analysis of a new fault-tolerant linear permanent-magnet motor for maglev transportation applications," IEEE Transactions on Applied Superconductivity, vol. 22, pp. 5200204-5200204, 2012.

[22] Y. Guo, J. X. Jin, J. G. Zhu, and H. Y. Lu, "Design and analysis of a prototype linear motor driving system for HTS maglev transportation," IEEE Transactions on applied superconductivity, vol. 17, pp. 2087-2090, 2007.

[23] T. W. Ching and W. Li, "A Superconducting Linear Variable Reluctance Machine for Urban Transportation Systems" IEEE Transactions on Applied Superconductivity, vol. 28, N. 3, Article#: 0601805, 2018.

[24] E.-J. Park, S.-Y. Jung, and Y.-J. Kim, "A Design of Optimal Interval between Armatures in Long Distance Transportation PMLSM for End Cogging Force Reduction," Journal of Electrical Engineering and Technology, vol. 11, pp. 361-366, 2016

[25] K. Suzuki, Y.-J. Kim, and H. Dohmeki, "Proposal of the section change method of the stator block of the discontinuous stator permanent magnet type linear synchronous motor aimed at long-distance transportation," in Electrical Machines, 2008. ICEM 2008. 18th International Conference on, 2008, pp. 1-6.

[26] Q. Lu, Y. Yao, Y. Ye, and J. Dong, “Research on ropeless elevator driven by PMLSM,” 2016, doi: 10.1109/EVER.2016.7476386.

[27] X. Huang, J. Liang, B. Zhou, C. Zhang, L. Li, and D. Gerada, “Suppressing the Thrust Ripple of the Consequent-Pole Permanent Magnet Linear Synchronous Motor by Two-Step Design,” IEEE Access, vol. 6, pp. 32935–32944, 2018, doi: 10.1109/ACCESS.2018.2847237.

[28] Z. Liu, X. Wang, B. Du, X. Xu, S. Ji, and C. Xiao, “Performance Optimization Analysis of PMLSM with Novel Composite Magnetic Slot Wedge,” 2019, doi: 10.1109/ICEMS.2019.8921716.

[29] T. Dong, R. Fu, B. Zhang, B. Peng, and X. Wei, “Analysis of Permanent Magnet Linear Synchronous Motor Made by Oriented Silicon Steel Sheet,” IEEE Transactions on Industry Applications, vol. 59, no. 3, pp. 3332–3340, 2023, doi: 10.1109/TIA.2023.3253816.

[30] M. Vatani and M. Mirsalim, “Comprehensive Research on a Modular-Stator Linear Switched Reluctance Motor with a Toroidally Wound Mover for Elevator Applications,” in 2019 10th International Power Electronics, Drive Systems and Technologies Conference, PEDSTC 2019, 2019, pp. 61–66, doi: 10.1109/PEDSTC.2019.8697241.